



OPEN ACCESS

EDITED BY
Shanfang Huang,
Tsinghua University, China

REVIEWED BY
Hui He,
Shanghai Jiao Tong University, China
Jinbiao Xiong,
Shanghai Jiao Tong University, China

*CORRESPONDENCE
Zhengyu Du,
✉ duzhy931004@163.com
Changhong Peng,
✉ pengch@ustc.edu.cn

SPECIALTY SECTION
This article was submitted to Nuclear Energy,
a section of the journal
Frontiers in Energy Research

RECEIVED 21 October 2022
ACCEPTED 28 December 2022
PUBLISHED 10 January 2023

CITATION
Liu Y, Huang M, Du Z, Peng C and Wang Z
(2023), Peak power prediction method of
heat pipe cooled reactor start-up and
power-up processes based on ANN.
Front. Energy Res. 10:1075945.
doi: 10.3389/fenrg.2022.1075945

COPYRIGHT
© 2023 Liu, Huang, Du, Peng and Wang.
This is an open-access article distributed
under the terms of the [Creative Commons Attribution License \(CC BY\)](https://creativecommons.org/licenses/by/4.0/). The use,
distribution or reproduction in other
forums is permitted, provided the original
author(s) and the copyright owner(s) are
credited and that the original publication in
this journal is cited, in accordance with
accepted academic practice. No use,
distribution or reproduction is permitted
which does not comply with these terms.

Peak power prediction method of heat pipe cooled reactor start-up and power-up processes based on ANN

Yu Liu¹, Mengqi Huang², Zhengyu Du^{1,2*}, Changhong Peng^{2*} and Zhe Wang³

¹Science and Technology on Reactor System Design Technology Laboratory, Nuclear Power Institute of China, Chengdu, Sichuan, China, ²School of Nuclear Science and Technology, University of Science and Technology of China, Hefei, Anhui, China, ³Nuclear and Radiation Safety Center of the Ministry of Ecology and Environment, Beijing, China

The start-up and power-up processes of the heat pipe cooled reactor are essential parts of the autonomous operations. The rapid power fluctuation in the processes can affect the safety of the heat pipe reactor. The fast and accurate prediction of the peak power is significant for the safe operation of the heat pipe cooled reactor. This paper generates the peak power datasets of heat pipe cooled reactor start-up and power-up processes by coupling Monte Carlo sampling, and system analysis program with heat pipe cooled reactor MegaPower as the research object. A fast prediction model of peak power was developed based on the artificial neural network and evaluated in terms of cost, accuracy, and interpretability. The results show that the artificial neural network model has high prediction accuracy and is suitable for large datasets with complex non-linear relations. However, the training cost is high, and the interpretability is weak. The above characteristics are explained by theoretical analysis, and the ability of ensemble algorithms to improve the accuracy of the artificial neural networks is discussed.

KEYWORDS

start-up, power-up, neural network, heat pipe cooled reactor, peak power

1 Introduction

The heat pipe cooled reactor is an advanced solid-state reactor whose core consists of a hexagonal stainless-steel monolith structure containing uranium-oxide (UO₂) fuel pins and heat pipes. As the core heat transfer component, the heat pipes carry away the core heat to the second loop or the thermoelectric conversion device in a non-energetic manner, eliminating pumps, valves, and auxiliary support systems. Hence, unlike traditional light water reactors, heat pipe cooled reactors are characterized by high inherent safety, compact structure, low operation pressure, long core life, and sound economy, and can be applied to particular scenarios such as deep-sea, space, and star surface. However, due to the small delayed neutron fraction, low matrix heat capacity, weak fuel, and matrix Doppler effects in heat pipe cooled

Abbreviations: ANN, artificial neural network; BP, back propagation; CANDU, CANada Deuterium Uranium; CFX, Computational Fluid X; HPRTRAN, Heat Pipe cooled Reactor TRANsient analysis code; MCNP, Monte Carlo N Particle; M-P, McCulloch and Pitts; MSE, Mean Square Error; NBDT, Neural Backed Decision Tree; RMSE, Root Mean Square Error; SCWR FA, Super Critical Water Reactor Fuel Assembly; STD, standard deviation.

reactor, it faces rapid variation in power with reactivity perturbations and temperature fluctuations.

The peak power is an essential factor affecting reactor safety, and reactors are generally designed with over-power protection devices to protect the reactor from over-power. Once the over-power protection signal is triggered, the reactor will shut down urgently. In most application scenarios, heat pipe cooled reactors must operate unattended for an extended period. In the face of load changes, the operating system needs to startup or mediate power to match the reactor power to the load while keeping the peak power in a reasonable range. Considering the rapid power variation of heat pipe cooled reactor, the implementation of this function relies on the accurate and fast prediction of the core power.

The reactor core power is generally obtained by the physical model based on the nuclear reaction mechanism or the analytical method of the experimental model. [Dias and Silva \(2016\)](#) used the neutron flux density method to infer the reactor power. However, the neutron flux density is not only related to the power level but also affected by the degree of fuel consumption. [Song \(2002\)](#) sensors outside the core to measure the power, but it is challenging to arrange sensors in some scenarios. The sensitivities of the sensors will also affect the accuracy of power estimation. Simple mathematical or physical models cannot accurately describe or estimate the nuclear reaction process due to a large number of non-linearities and uncertainties involved.

Numerical simulation of the phenomena in the reactor by coupling the thermohydraulic and neutronics models is another means. [Xi et al. \(2013\)](#) analyzed the axial power distribution of the European supercritical water-cooled reactor SCWR FA by coupling the thermohydraulic code CFX and the neutronics code MCNP. Although the best estimation procedure provides accurate results, it does not meet the requirements for autonomous operation in remote due to a large amount of computation time.

With the development of machine learning techniques, the use of data-driven models to predict the trends of critical parameters in real-time based on the feature parameters plays an increasingly active role in the safe operation of nuclear power plants. [Bae et al. \(2021\)](#) proposed a data-driven model consisting of a multi-step prediction strategy and an artificial neural network, which can help the operators estimate the trend of parameters under emergencies to respond quickly to the current situation.

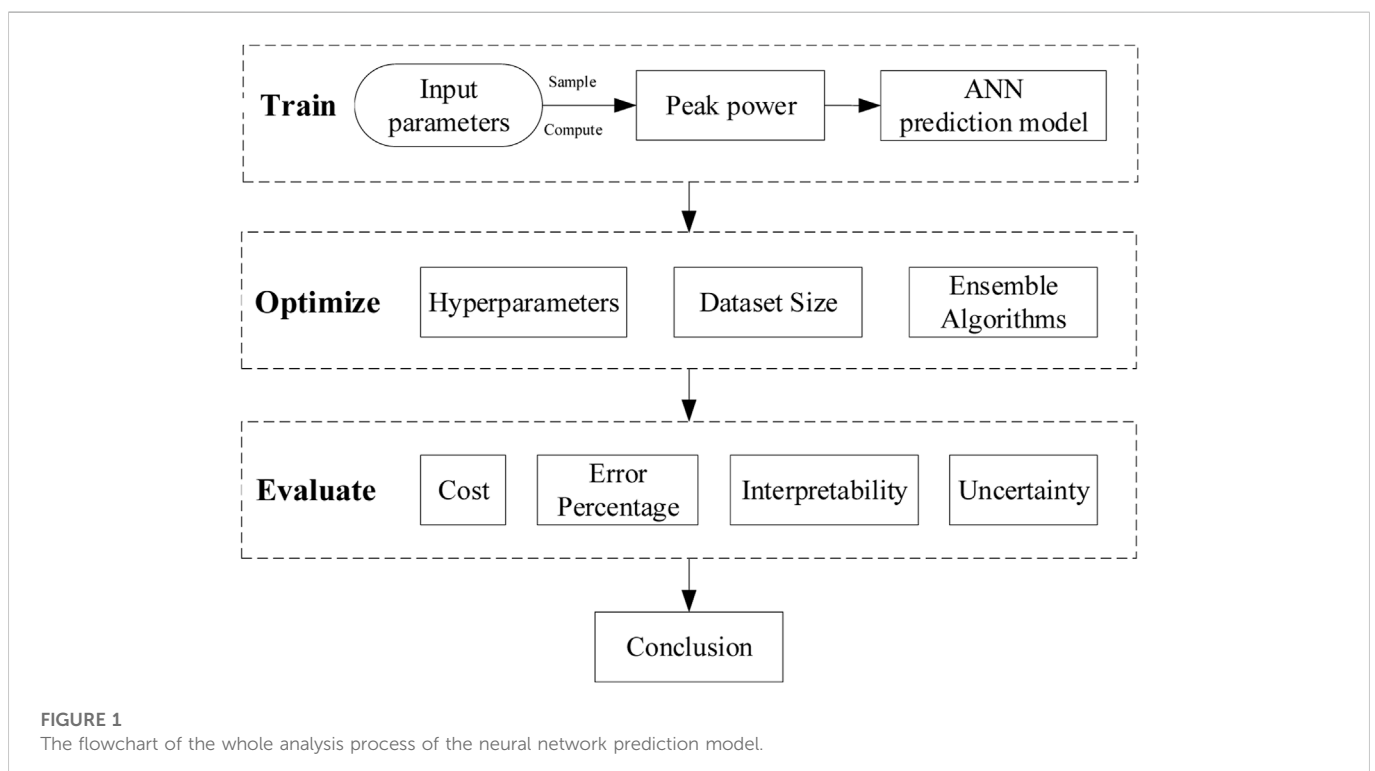
Given the data-driven model's excellent performance, this study try to apply it to the field of power prediction. This paper takes MegaPower, a heat pipe cooled reactor designed by Los Alamos National Lab for strategic power supply in remote as the subject ([Sterbentz et al., 2017](#)). Firstly, a model based on an artificial neural network to predict the peak power of heat pipe cooled reactor start-up and power-up processes is built. Then ensemble approaches are used to optimize the prediction performance further. After that, the applicability of this model is analyzed. [Figure 1](#) shows the entire analysis flowchart of this article.

2 Problem introduction and dataset

2.1 Problem introduction

MegaPower is a heat pipe cooled reactor designed by Los Alamos National Lab for strategic power supply in remote ([Mcclure et al., 2015](#); [Sterbentz et al., 2017](#)). [Figure 2](#) shows some of the major reactor structures.

The core consists of a hexagonal stainless-steel monolith structure containing 5.22 Mt of uranium-oxide (UO₂) fuel pins and liquid metal potassium (K) heat pipes operating at 675°C. By vaporizing the potassium liquid in the heat pipes, the heat pipes remove heat from the monolith; no pumps or valves are needed. Heat is then



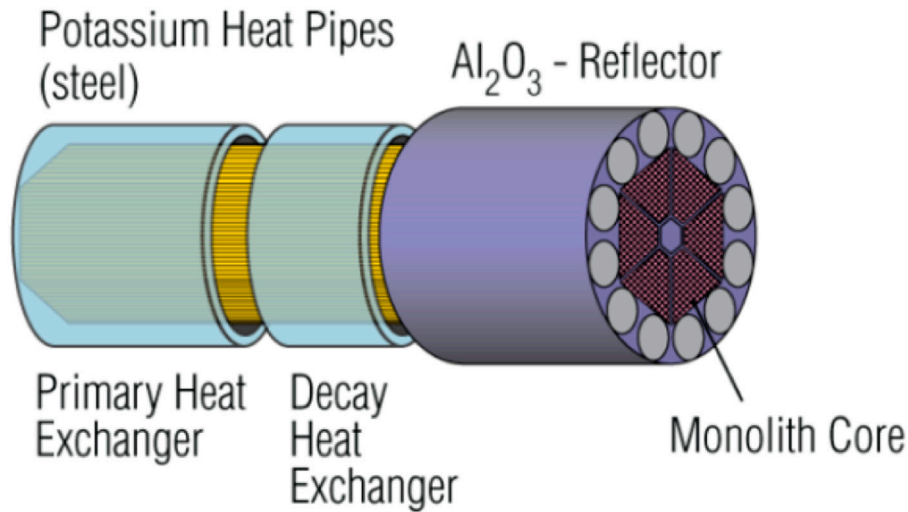


FIGURE 2 Concept schematic of heat pipe cooled reactor MegaPower (Sterbentz et al., 2017).

deposited in the condenser region of the heat pipe. Condenser regions can accommodate multiple heat exchangers. Reaction control is achieved using alumina (Al_2O_3) neutron side reflectors with 12 embedded control drums containing boron-carbide (B_4C) poison arcs.

The heat pipe cooled reactor increases reactivity by rotating the control drum. Zhong et al. (2021) have proposed a “frog-hopping” power control strategy to improve the safety of the heat pipe cooled reactor in the power mediation process. As shown in Figure 3, the system is as follows.

During the start-up process, when the reactor is critical, after each rotation of the control drum, if the change of the reactor power and the average fuel temperature is within limits during the subsequent observation time, the reactor is considered to be in a controllable state, and the control drum is continued to be rotated. Otherwise, the control drum is stopped until the conditions are satisfied again. In the power-up process, it is necessary to wait some time to perform the following operation after reaching the current power.

Therefore, the main operation parameters affecting the target parameters and their value ranges and distributions were identified, as shown in Table 1. During the process of reaching the target value of the core power, there is an urgent need to know the effect of the parameters on the power, as the different rotation patterns of the control drum may lead to a huge variation of the transient power. Model-based, knowledge-based, and data-driven methods are commonly used for prediction. However, the model-based method has a longer calculation time, the knowledge-based method has little empirical knowledge, and only the data-driven method can overcome the problems in peak power prediction.

2.2 Dataset

Although the data-driven method has shown promising applications, its performance is influenced by the quality of the

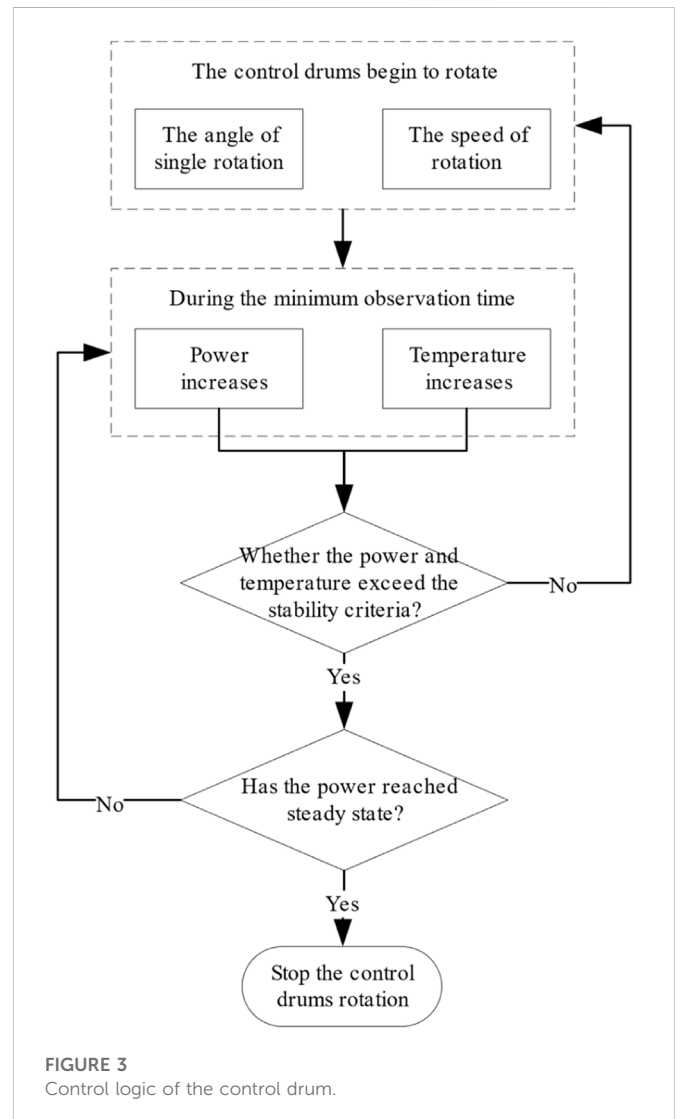
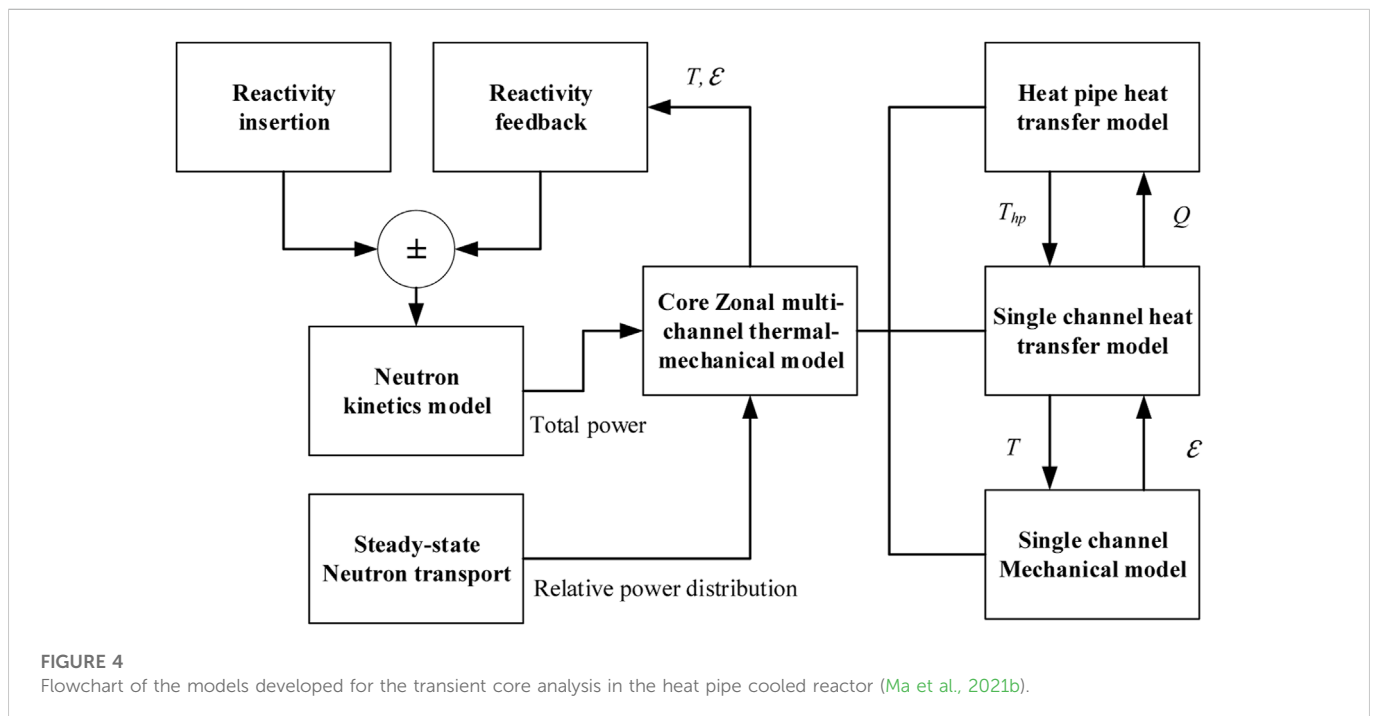


FIGURE 3 Control logic of the control drum.

TABLE 1 The range and distribution of the input parameters in start-up and power-up processes.

Parameter	Acronym	Range	PDF	Process applied to
The angle of a single rotation	ASR	$[0.5,5.5]^{0.5}$	Discrete	Start-up and power-up
The speed of rotation	SR	$(10,60)^{\circ}/\text{min}$	Uniform	Start-up and power-up
The minimum observation time	MOT	$(1,20)\text{s}$	Uniform	Start-up and power-up
The power stability criteria	PSC	$(1,30)\text{K}$	Uniform	Start-up and power-up
The temperature stability criteria	TSC	$(0.003,0.1)$	Uniform	Start-up and power-up
Initial power factor	IPF	$(0.0,1.0)$	Uniform	Power-up
Target power factor	TPF	$(0.0,1.0)$	Uniform	Power-up
Delay time	DT	$(11,000)\text{s}$	Uniform	Power-up

Note: "Initial power factor" donates the relative power before the power-up process, "Target power factor" donates the relative power after the power-up process, "the relative power" donates the ratio of power to full power.



data. In practice, obtaining reliable training data is difficult, which relies on effective procedures. The HPRTRAN is a heat pipe cooled reactor system analysis code developed by the Nuclear Power Institute of China, consisting of a point reactor kinetics model, a reactivity feedback model, a core heat transfer and mechanical model, and a heat pipe model (Ma et al., 2021a).

Figure 4 shows the flowchart of the models in the HPRTRAN code. The neutronic kinetics model determines the total power with the neutron transport simulation to obtain the relative power distribution. Thermal-mechanical calculations are carried out with the transferred power. There are three components to the core multi-channel thermal-mechanical model: a heat pipe model, a single channel coupled thermal-mechanical model, and a radial heat transfer model. Using the heat pipe model, the evaporator outwall temperature and the monolith's inner wall temperature are determined. By transferring the thermal expansion and temperature

distribution from the core thermal-mechanical model to the neutron kinetics model, the reactivity feedback can be considered.

The reasonability and feasibility of the models were verified by comparing the computational results of the HPRTRAN code with the ANSYS code and experimental results (Ma et al., 2021b; Ma et al., 2022).

HPRTRAN can well simulate the heat pipe reactor in the start-up and power-up processes. Taking the start-up process as an example, the system parameters, including core geometry parameters, power distribution, reactivity feedback, etc., are initialized, followed by transient calculations, where the point kinetic equations, core multi-channel heat transfer model, and heat pipe model are solved explicitly; The core internal reactivity is determined from the fuel, monolith, heat pipe, and reflector operating temperatures, and summed with the external reactivity introduced by the control drum as the total reactivity. Update the temperature field and the

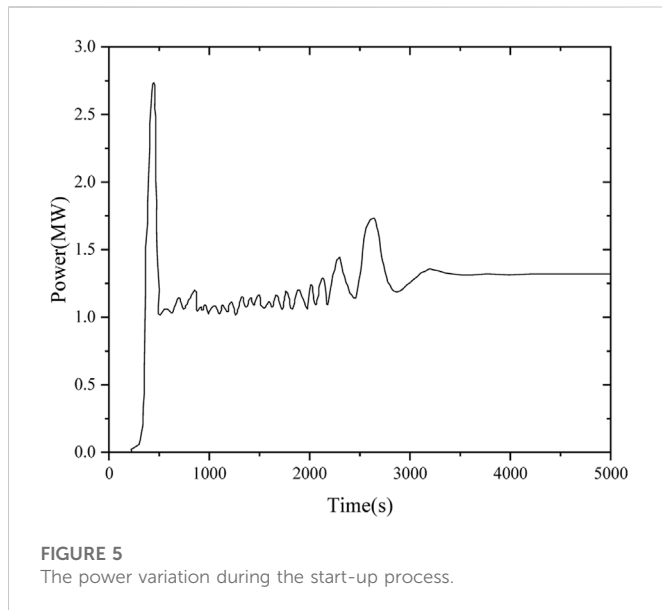


FIGURE 5
The power variation during the start-up process.

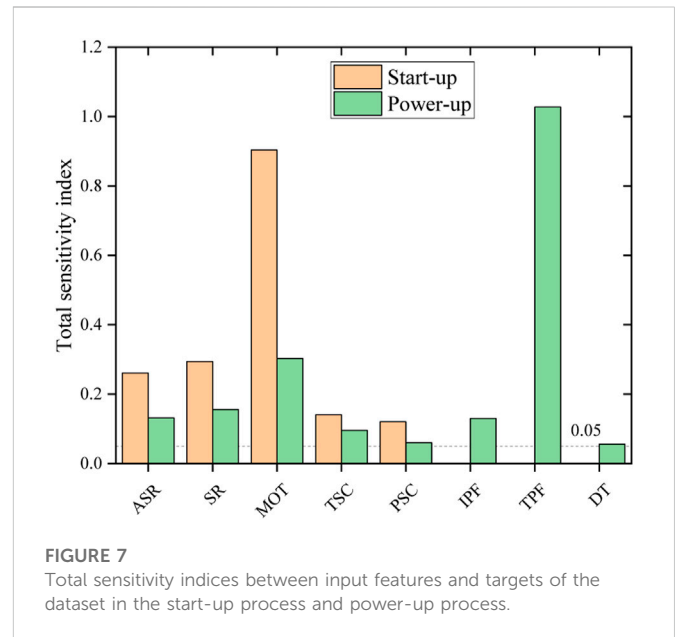


FIGURE 7
Total sensitivity indices between input features and targets of the dataset in the start-up process and power-up process.

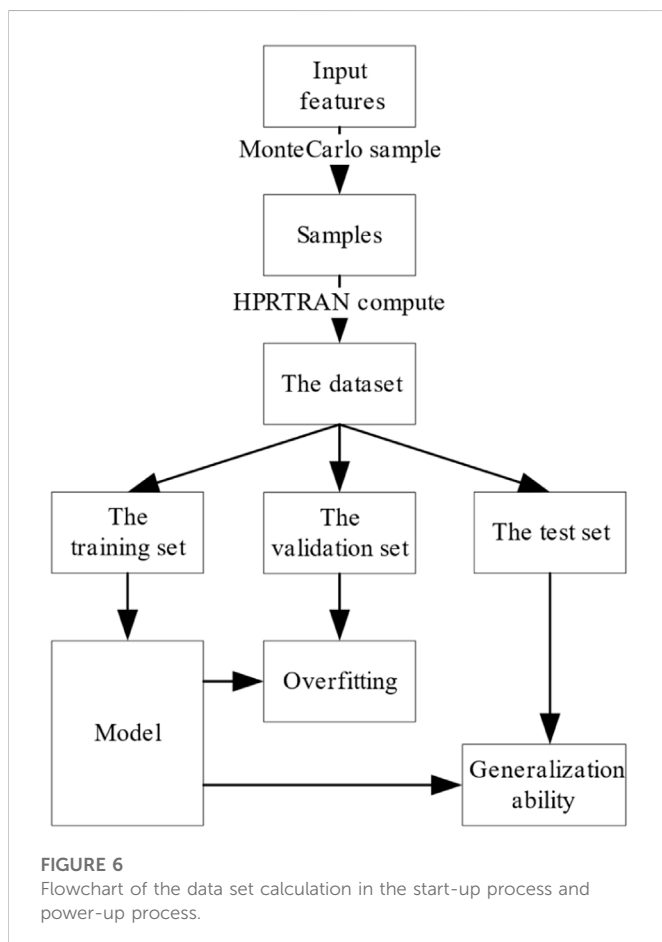


FIGURE 6
Flowchart of the data set calculation in the start-up process and power-up process.

heat transfer between channels. Multiple iterations are performed until the preset calculation time is reached. Figure 5 shows the power variation during the start-up process (Ma et al., 2021a).

As shown in Figure 6, a Monte Carlo simulation is performed for the input parameters of the process of start-up and power-up, respectively. The influence of the input parameters on the target

parameters is calculated using HPRTRAN to obtain the dataset containing the input features and the target values. The dataset size for both the start-up and power-up processes is 2000.

The dataset is divided into a training set, validation set, and test set according to the ratio of 3:1:1. The training set is used to train the prediction model and calculate the model's parameters. The validation set determines whether the model is underfitting or overfitting. The test set is used to check the model generalization performance.

The model uses the root mean square error (RMSE) between the predicted and actual values of the target parameters as the evaluation metric, as shown in the following equation.

$$RMSE = \sqrt{\frac{1}{N} \sum_{i=1}^N [(f_i^{predict} - f_i^{true})^2]} \quad (1)$$

Sobol sensitivity analysis is based on the variance decomposition technique. It is suitable for measuring the non-linear relationship between multiple input parameters and outputs (Ikonen, 2016), selecting a total sensitivity index value of 0.05 as a distinction between important and unimportant parameters (Zhang et al., 2015). Figure 7 shows the Sobol sensitivity index between the input parameters and the target values in the dataset. The results show that although there are differences in the sensitivity indices of each input feature, they satisfy the requirements of the critical parameters, and there are no redundant features.

3 Regression model

This section introduces the neural network algorithm and three ensemble algorithms.

3.1 Neural network

The neuronal action potential will change when a stimulus is delivered to a neuron in the human brain. If the potential exceeds a

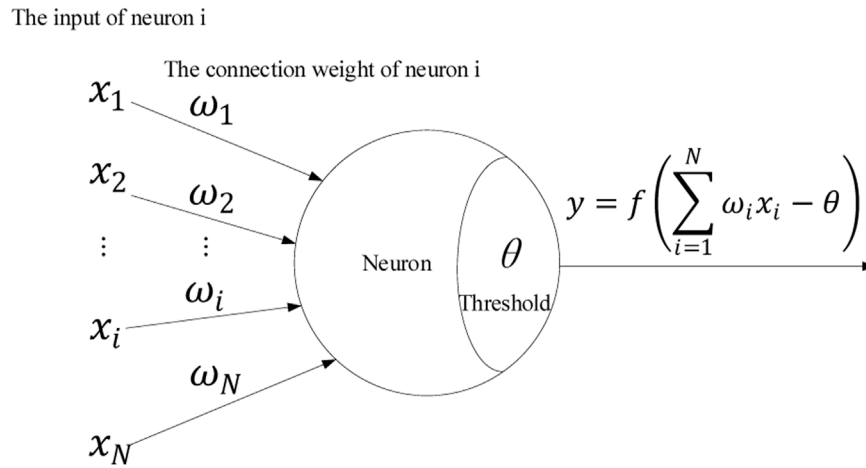


FIGURE 8
Concept schematic of the M-P neuron model.

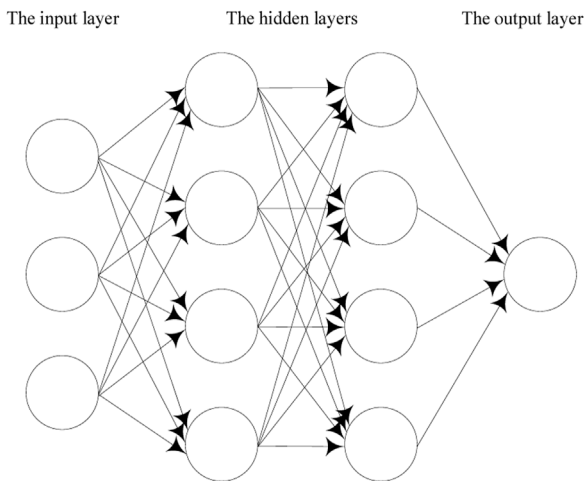


FIGURE 9
Concept schematic of the fully connected artificial neural network model.

threshold, the neuron is activated and sends neurotransmitters to other neurons. The artificial neural network (ANN) is built concerning the structure of the human brain nervous system. The M-P neuron shown in Figure 8 simulates the neuron in the human brain. The M-P neuron receives the input x_i from other neurons, multiplies it by the connection weight ω_i , and then subtracts the activation threshold θ to obtain the output value $\sum \omega_i x_i - \theta$. The non-linear activation function f transforms the original output value to consider the non-linear factor.

As shown in Figure 9, the artificial neural network consists of an input layer, several hidden layers, and an output layer. Each layer includes several M-P neurons. The data are propagated backward and forward, but no co-layer and cross-layer propagation occur.

The neural network optimizes the parameters ω and θ of the neurons using the error back propagation algorithm (BP). The BP algorithm updates the parameters through stochastic gradient descent and can step out of the local optimum values and find the optimum global value.

TABLE 2 Training and prediction time of the neural network model.

The dataset	Training time s)	Prediction time(s)
S (E)art-up	120.1635	5.8364-3
Power-up	139.3435	6.0854-3

TABLE 3 Partial hyperparameters of the neural network.

Type of hyperparameters	Hyperparameter
Network structure	n_dense
	n_hidden
Model training	epochs
	batch_size
	earlystopping
	loss
	activation
	optimizer
	initialization
	regularization
	standardization
learningrate	

4.2 Model evaluation

This section provides a comprehensive evaluation of the neural network prediction model in terms of cost, accuracy, interpretability, and uncertainty.

4.2.1 Cost

The artificial neural network has many parameters. There are corresponding connection weights between neurons of adjacent two

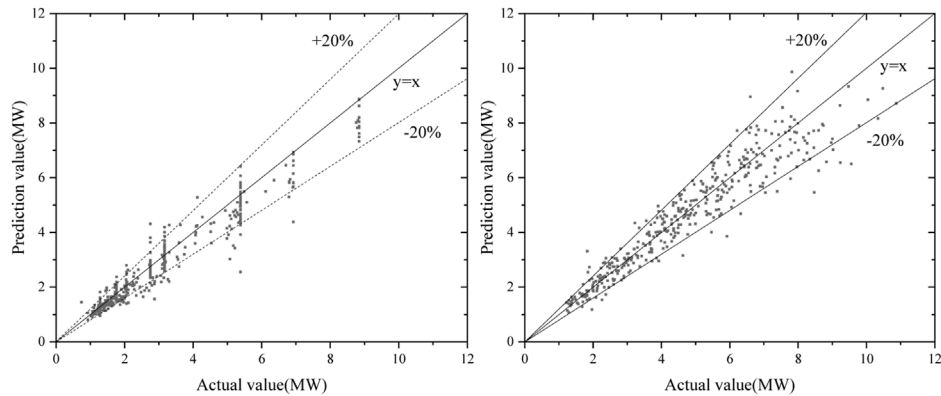


FIGURE 10

Error percentage distribution of test set prediction by the neural network during the start-up process and power-up process.

layers and thresholds on each. The artificial neural network adopts the BP algorithm to update parameters, which requires the input to be propagated layer by layer from front to back. Then the error is propagated step by step from back to front. It takes a long time to train the artificial neural network model. Table 2 shows the time required to prepare and predict the neural network model on the two datasets.

The complexity of the neural network model is also reflected in the size of the model hyperparameters. Table 3 shows part of the hyperparameters of the neural network.

The model's generalization performance can be driven to the best state by adjusting the values of hyperparameters. Due to a large number of hyperparameters, it usually takes time to adjust the parameters of the neural network. Thus, it is more sensible to select the random sampling method in tuning the neural network model.

4.2.2 Error percentage

The peak powers of the test set were predicted using the optimized neural network model, and the error percentage distributions are shown in Figure 10.

The error percentages of the neural network are within 20% in both the start-up and the power-up processes, showing the high accuracy of artificial neural networks. There are two reasons. One is that the neural network has lots of parameters that can fit complex functional relations. Hornik (1991) has proved that, under certain conditions, the artificial neural network is capable of arbitrarily accurate approximation to a function. Secondly, in updating the model parameters, the neural network uses the stochastic gradient descent algorithm; it can jump out of the local extremes and find the global minimum.

4.2.3 Interpretability

Talking about the interpretability of models, an eural network is more of a black box in that it delivers results without an explanation. It is only possible to observe what caused the neuron's activation on the first hidden layer and what the neuron's activation did on the last hidden layer. It is difficult to understand more neurons in the hidden layers in the middle. Therefore, the neural network is unsuitable for some scenarios requiring high interpretability.

The interpretability of neural networks is currently a research hotspot, which can be divided into active and passive interpretability studies according to whether interpretability interventions are made in the design and training processes of the model. Active interpretation drives neural network models in the direction of interpretability by adding physical information to the structure of the model, using physical constraints in the model's training process, or combining the neural network with other models with high interpretability. Wan et al. (2020) constructed the neural-backed decision tree NBDT by replacing each node in the decision tree with a neural network, claiming it preserves the high precision of a neural network and high-level interpretability of a decision tree and successfully applied in the field of image recognition. However, due to the specific modification of the internal structure of the neural network by active interpretation, it is less intuitive in interpretation and has a narrow scope of application. Therefore, more work is currently focused on passive interpretation.

In this section, the neural network prediction models are interpreted using the attribution interpretation and the distance interpretation, respectively, according to the decreasing interpretability completeness.

4.2.3.1 Attribution interpretation

The concept of attribution interpretation refers to the attribution of responsibility or blame based on the effects of the input features on the output. The rapid rotation of the control drum brings about a rapid rise in core temperature and the following negative temperature feedback, so the total reactivity fluctuates violently near the criticality, generating power fluctuations and the maximum peak power.

Figure 7 shows the contribution of the input features to the peak power, during the start-up process, with the minimum observation time having the most significant effect on the peak power, followed by the control drum's angle of a single rotation and speed of rotation. At the microscopic level, the single rotation angle and rotation speed of the control drum directly affect the speed of each control drum rotation. Thus, the contribution to the peak power is enormous. At the macroscopic level, the minimum observation time determines the length of the single rotation interval of the control drum during the "frog-hopping" start-up. Actually, it controls the overall speed of the control drum during the whole rotation.

TABLE 4 Attribution interpretation of the peak power prediction model in the power-up process.

Number	ASR	SR	MOT	TSC	PSC	Predict peak power
1	0.90	0.50	0.16	0.43	0.07	1,535,104
2	0.90	0.28	0.95	0.81	0.22	1,581,559
3	0.80	0.84	0.68	0.19	0.14	1,697,292
4	0.90	0.82	0.74	0.25	0.21	1,847,500
5	1.00	0.22	0.26	0.50	0.30	1,989,466
6	0.50	0.98	0.32	0.18	0.53	3,193,530
7	0.30	0.06	0.32	0.30	0.59	3,565,175
8	0.90	0.20	0.21	0.72	0.47	4,817,171
9	0.20	0.46	0.05	0.24	0.52	5,491,084
10	0.60	0.18	0.53	0.94	0.85	5,848,254

In the power-up process, the target power factor becomes the most influential factor on the peak power, which is well understood as it determines the steady-state power level and, naturally, the peak power range above the steady-state power.

The above analysis illustrates the usefulness of analyzing the effect of input features on the peak power according to Figure 7. This section takes the power-up process as an example to perform the attribution interpretation by sampling ten samples from the test set. All the samples are normalized and sorted by the output value. As shown in Table 4, it is easy to identify the features that contribute most on the peak power when it is small or large. For instance, the small PSC value in sample No. 1 limits the speed of power increase. And the large MOT values in samples No. 2–4 extend the rotation interval of control drum. All the above factors reduce the reactivity introduction speed. The large peak powers of samples No. 8–10 come from the opposite reason.

The attribution interpretation explains the results from the mechanism, which can deepen the understanding of the peak power formation process, but it requires human confirmation in practice, which is inconvenient. Therefore, this section adopts the distance interpretation method based on Euclidean distance to prove the reliability of the model prediction results.

4.2.3.2 Distance interpretation

The distance interpretation finds the nearest training sample from the training set to explain the output for a particular test sample. A reasonable assumption is that the peak power is considered a function of the input features and that the “derivatives” are present and bounded over most of the domain so that the outputs of the test sample and the nearest training sample should not be too different from each other.

Therefore, this section still selects the above 10 test samples, searches for the nearest training samples and compares their outputs. The results are shown in Figure 11. It is found that the output values of five nearest training samples are within the 20% error range of test samples, indicating that the output of the neural network can be quickly verified by distance interpretation.

4.2.4 Uncertainty

The uncertainty of the model contains epistemic uncertainty and aleatory uncertainty, where the epistemic uncertainty comes from the

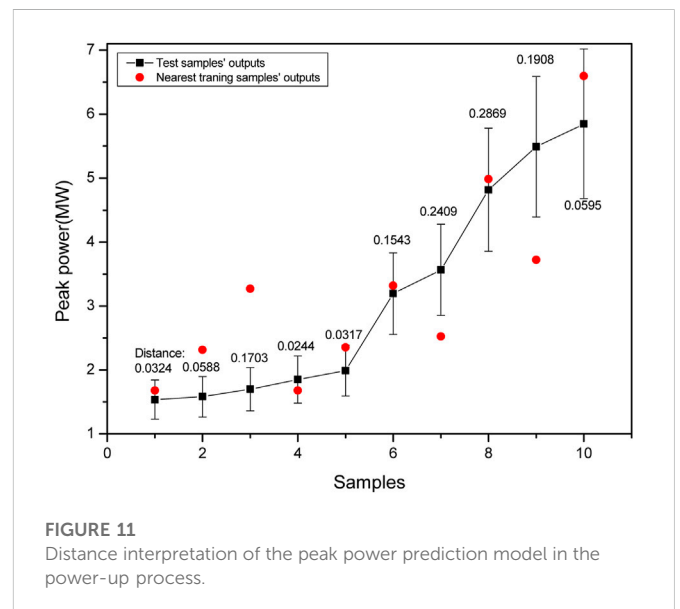


FIGURE 11 Distance interpretation of the peak power prediction model in the power-up process.

lack of understanding of the physical system, and aleatory uncertainty comes from the uncertainty of the physical system itself, which is difficult to distinguish in practice. This section analyzes the uncertainty of neural network models by identifying the sources of uncertainty, performing uncertainty propagation, and finally analyzing the output uncertainty.

The uncertainty of neural network comes from the model hyperparameters, training data, and model parameters. The model hyperparameters and training data are controllable uncertainties and can be specified artificially before training. The model parameters are uncontrollable uncertainties, which are updated by the gradient descent method during the training process and cannot be interfered with artificially, so the uncertainty of the model parameters can be considered by adding a Dropout layer to abandon the model parameters randomly (Gurgen, 2021). The process of model uncertainty quantification is shown in the Figure 12.

The uncertainty of the model is propagated through the framework shown in Figure 12. And it is then quantified by

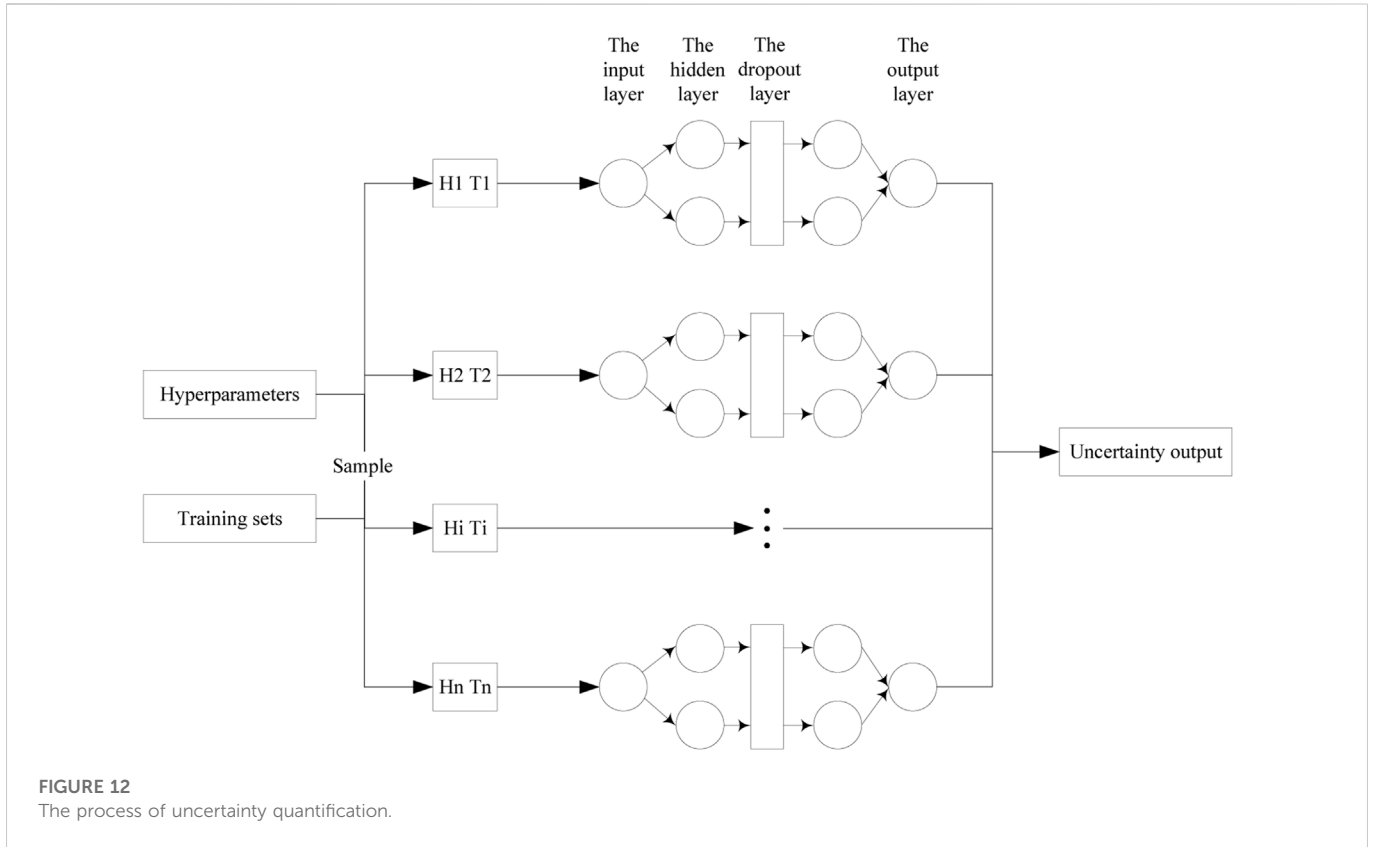


FIGURE 12
The process of uncertainty quantification.

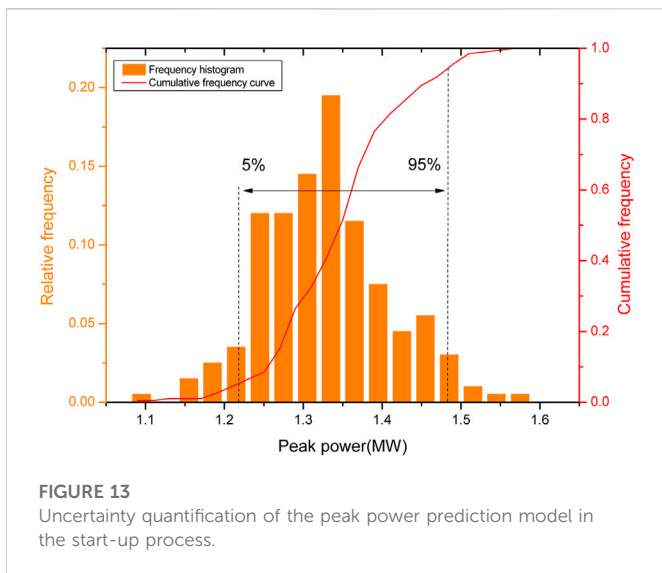


FIGURE 13
Uncertainty quantification of the peak power prediction model in the start-up process.

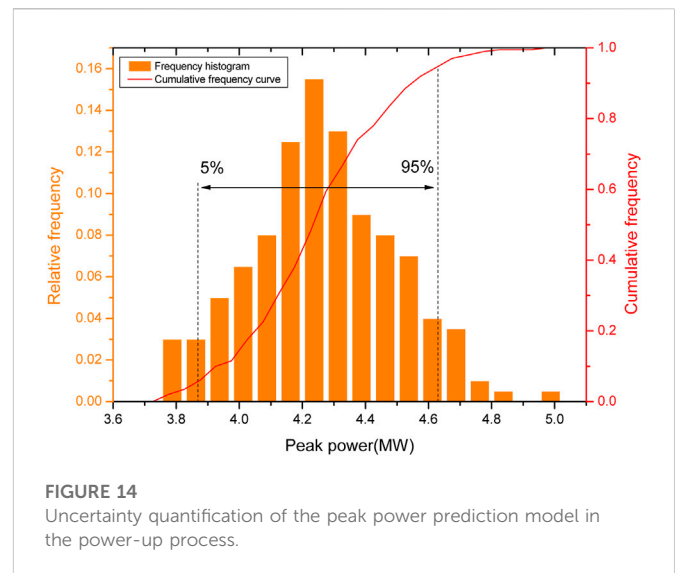


FIGURE 14
Uncertainty quantification of the peak power prediction model in the power-up process.

analyzing the uncertainty output. Taking a sample of the start-up process and the power-up process as an example respectively, the uncertainty outputs of the models are shown in Figures 13, 14.

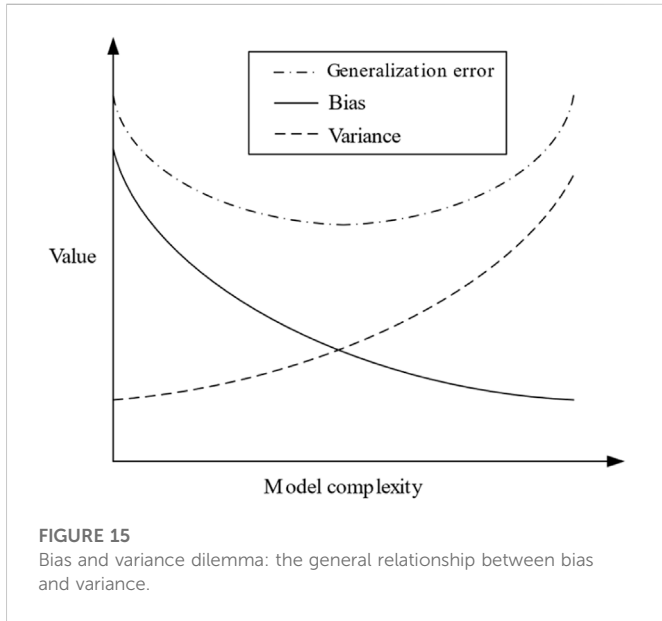
3.2 Ensemble algorithms

The predictive ability of a regression model for unknown samples is defined as the generalization error, expressed as the mean square

error (MSE) of the predicted and actual values of the target parameter. The mean square error (MSE) can be broken into two components: bias and variance.

$$MSE = Bias^2 + Variance \tag{2}$$

The bias indicates the accuracy of the model prediction, and the variance measures the stability of the prediction. The general relationship between bias and variance is shown in Figure 15 (Geman and Bienenstock, 1992).

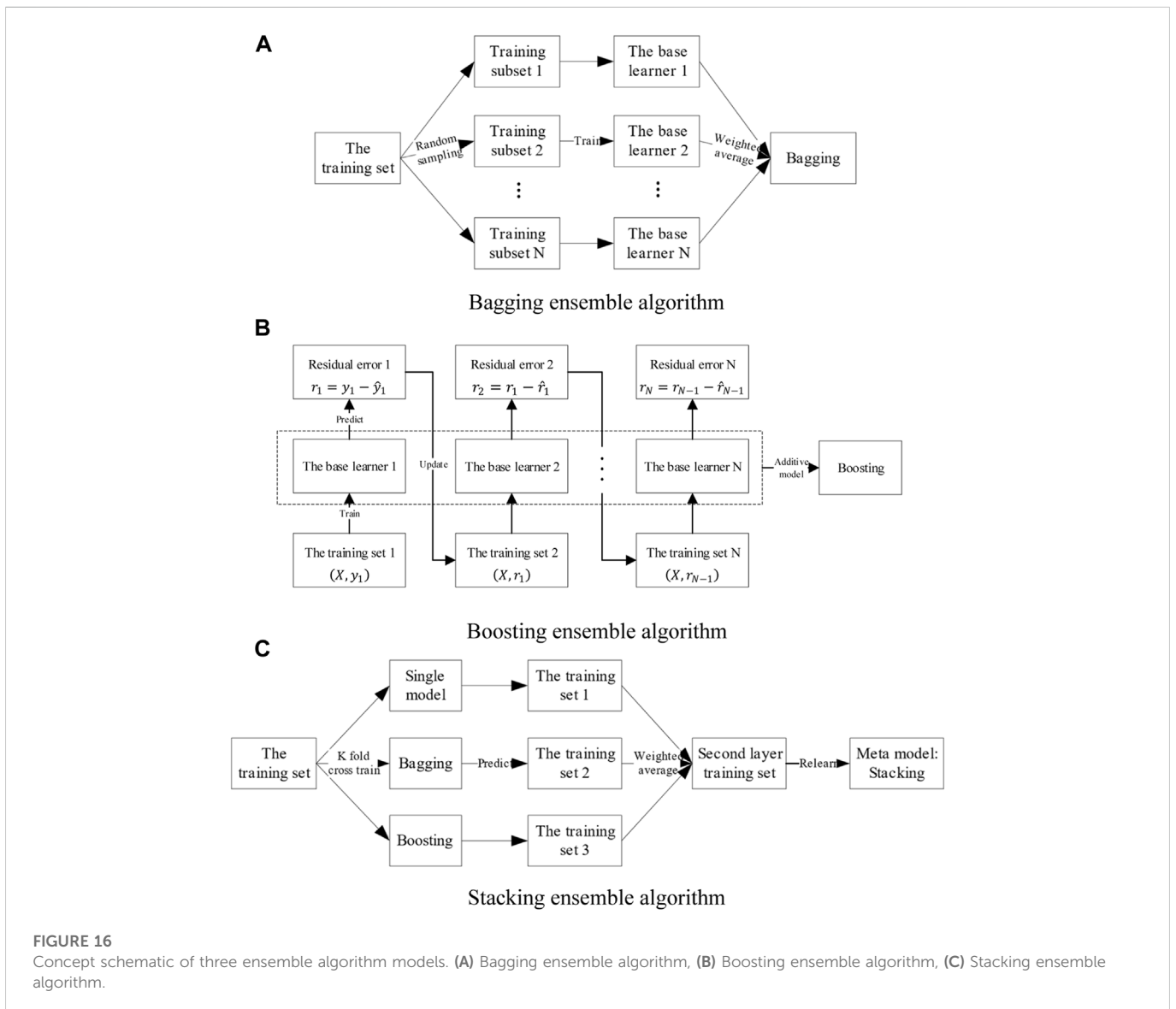


Zhou (2016) offers theoretical justification for ensemble algorithms that can improve the accuracy and stability of models and reduce generalization errors by enhancing the diversity of models. The conventional ensemble algorithms include bagging, boosting, and stacking based methods.

Bagging can reduce the variance of the ensemble model by sampling the dataset, training multiple regression models of the same type separately, and weighting the prediction results of the models to obtain the final output. Boosting uses the next model to predict the residuals of the previous model. Finally, it combines the prediction results of multiple weak regression models with an additive model, which can reduce the bias of the ensemble model.

Stacking has a two-layer structure, using different regression models to predict the dataset in the first layer and the prediction results as the dataset to train the meta-model in the second layer. Relearning the prediction results may obtain higher generalization performance.

This paper uses three ensemble algorithms to optimize the neural network, with the structure shown in Figure 16.



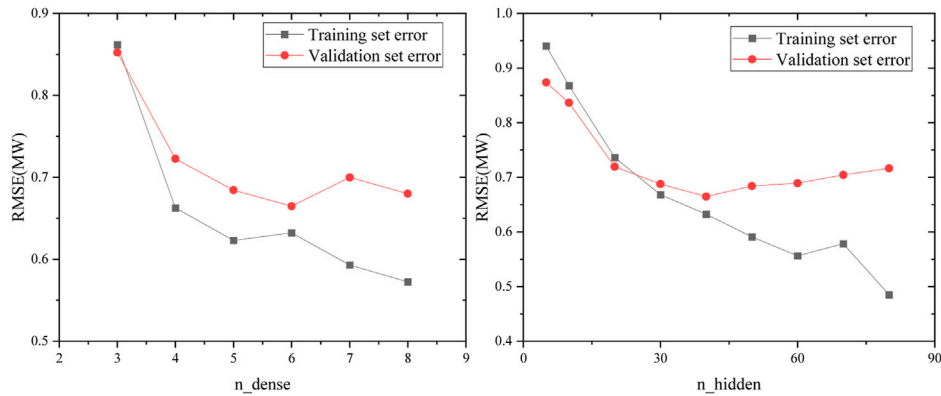


FIGURE 17
Influence of the neural network depth and width on overfitting.

4 Optimization and evaluation of artificial neural network model

The artificial neural network can model non-linear relationships between variables. Macroscopically, it partitions the data space by progressive decomposition and relies on the scale of the model to obtain better performance. The artificial neural network has a wide range of applications. However, the relationship between targets and features varies so much in datasets of different scenarios that it is difficult to use the comparative results on one dataset as a guide to another. This paper is more interested in how the ANN performs in the specific application scenario of the heat pipe cooled reactor’s start-up and power-up processes and how to comprehensively evaluate the neural network’s applicability.

Therefore, this section builds a peak power prediction model for the heat pipe cooled reactor’s start-up and power-up processes based on an artificial neural network, optimizes the model by adjusting the model structure, and evaluates the model’s performance in terms of cost, accuracy, interpretability, and uncertainty using a comprehensive framework.

4.1 Model optimization

The accuracy of neural network models is affected by numerous factors. The hyperparameters affect the prediction ability by determining the complexity of the model, the training data directly affect the effect of model learning, and the ensemble algorithms can achieve performance improvement through the combination of multiple models.

4.1.1 Hyperparameters optimization

The hyperparameters determine the complexity of the model. The learning ability of a simple model is limited, but as the complexity increases, the model overfits, i.e., gradually learns some properties of the training set and loses good generalization performance. Taking the power-up dataset as an example, the complexity of the model can be represented by hyperparameters that indicate the model structure size, such as the depth (n_dense) and width (n_hidden). The neural network

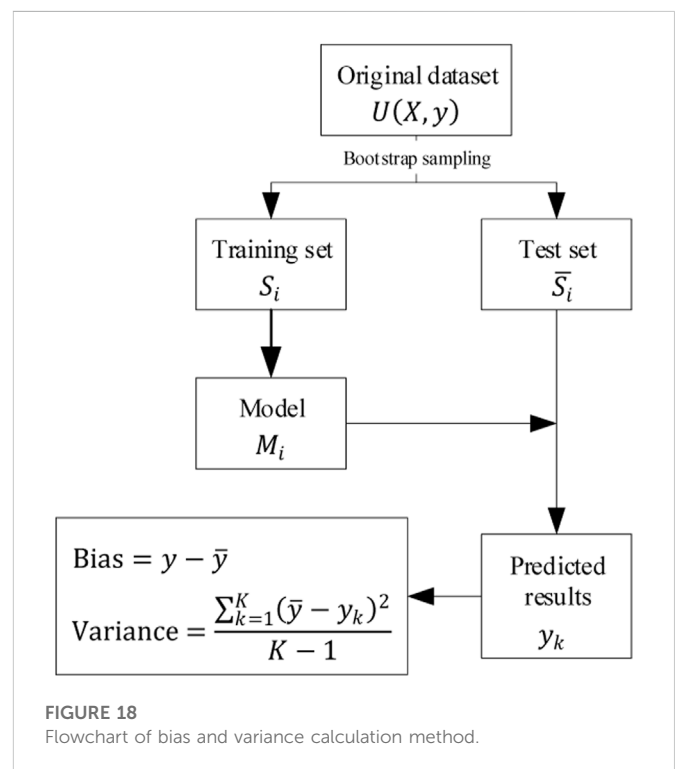


FIGURE 18
Flowchart of bias and variance calculation method.

will directly determine the size of the model. This section uses the training set to calculate the model parameters and the validation set to determine the degree of overfitting. Figure 17 shows the effect of hyperparameters on the overfitting of the neural network model.

The overfitting phenomenon can be observed in the training of the neural network. Although each neuron can use the complete samples, the increase in width due to the different weights still causes the effect of further division of the data space. The neural network that is too deep may cause parameters instability with vanishing gradient problems or exploding gradient problems due to the continued multiplication of multiple activation functions. Therefore, the hyperparameters should be tuned to alleviate the overfitting situation to get the prediction model with the best results.

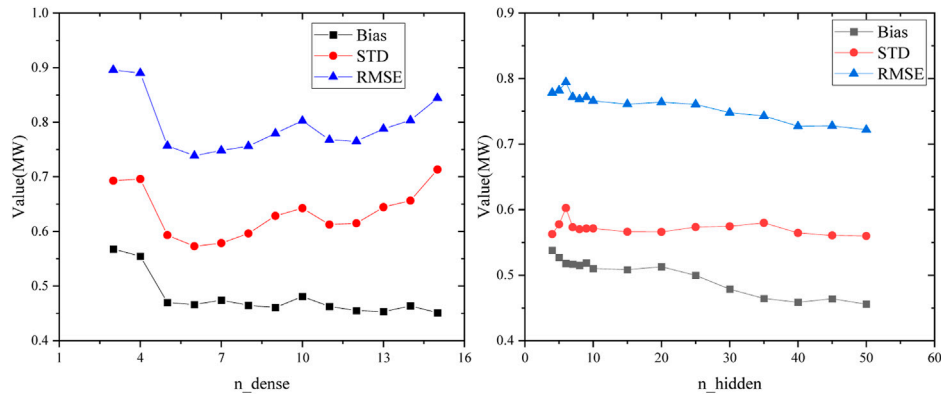


FIGURE 19
Influence of the neural network depth and width on bias and variance.

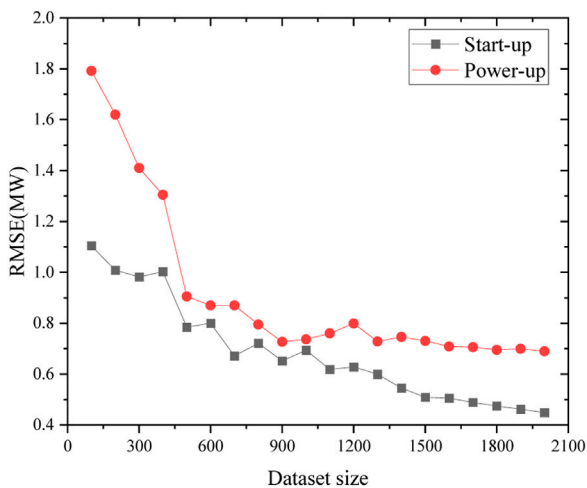


FIGURE 20
Influence of dataset capacity on RMSE in start-up and power-up processes.

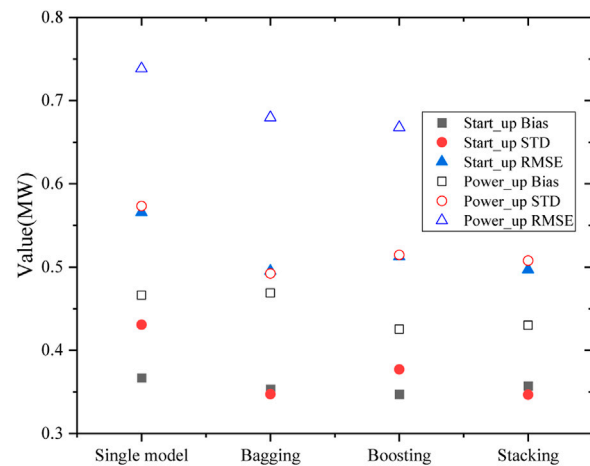


FIGURE 21
Effect of ensemble models in start-up and power-up processes.

This overfitting phenomenon of the model can be explained by the bias-variance dilemma, where the model complexity makes a difference in the effect of the bias and variance, thus leading to a change in the generalization error of the model, as shown in Figure 15. A model’s generalization error can always be decomposed into bias and variance, and the effect of hyperparameters on overfitting is a combination of the effects on bias and variance, respectively. The bias and variance are averaged over all possible datasets computed by the model and are only relevant to the model and not to the specific dataset.

In cases where datasets are difficult to obtain, the bias and variance of the model can be computed on the multiple datasets obtained by bootstrap replicates from the original dataset as shown in Figure 18 (Sofus et al., 2008).

Overfitting can be alleviated by adjusting the model hyperparameters and controlling the bias and variance in a suitable position. It is found that the bias of the neural network always decreases monotonically with the increase of depth or width. However, as the width increases, the variance is

unimodal, and it is found that deeper models increase variance. Thus, the trend of the generalization error of the neural network with model complexity depends on the relative magnitude of bias and variance (Yang et al., 2020).

The artificial neural network is a low bias but high variance model and the generalization error depends mainly on the control of variance. For the neural network, the variance will increase if the model is too deep. The effect of width on variance is still unimodal, as shown in Figure 19, and performance can be further improved by widening.

4.1.2 Dataset size

This section investigates the effect of dataset size on model error. Figures 20, 21 shows that the relationship between dataset size and model error has basically converged during the start-up and power-up processes, indicating that it is appropriate to use both datasets to train the neural network model. However, both datasets still have room for expansion to reduce the error. The neural network has many parameters. It is difficult for a small amount of data to learn more accurate parameters in the error back propagation process, so it is usually suitable for large datasets such as picture and text recognition.

4.1.3 Ensemble algorithms

Finally, the performance improvements of the three ensemble algorithms on the neural network model were compared. The results show that all three ensemble algorithms effectively reduce the generalization error of the models compared to single models.

The reduction effect on the variance and the bias is consistent with the theoretical analysis, with Bagging mainly reducing the variance and Boosting mainly reducing the bias. Considering that the neural network is a high variance but low bias model, the gains are more significant using Bagging than Boosting. While Stacking may obtain better results by relearning based on a simultaneous ensemble of a single model, Bagging and Boosting simultaneously.

5 Conclusion

The following research has been conducted in this paper. Firstly, the Monte Carlo sampling method and the deterministic model are combined to generate the heat pipe cooled reactor datasets in start-up and power-up processes. Then, the peak power prediction model based on the artificial neural network is established. Next, the influence of hyperparameters, dataset size, and ensemble algorithms on the model performance is studied. Finally, the following conclusions were obtained.

- (1) The neural network model has a high prediction accuracy. The prediction error of the peak power in the heat pipe cooled reactor is 0.5658 MW for the start-up process and 0.7385 MW for the power-up process. It has a low uncertainty, and the predictive percentage errors of most samples are less than 20 percent.
- (2) The neural network is a model with high variance and low bias. Thus, ensemble algorithms are mainly used to improve performance by reducing the variance of the model. The dataset size also impacts the model, and there is room for further expansion.
- (3) The training and tuning costs of the neural network are high; the training time is 120 s on the start-up process dataset and 139 s on the power-up process dataset. But it has a relatively low prediction cost. The interpretability is weak too. It can be partially explained by passive interpretation, such as attribution interpretation and distance interpretation. It could be improved by combing neural

References

- Bae, J., Kim, G., and Lee, S. J. (2021). Real-time prediction of nuclear power plant parameter trends following operator actions. *Expert Syst. Appl.* 186, 115848. doi:10.1016/j.eswa.2021.115848
- Dias, A. M., and Silva, F. C. (2016). Determination of the power density distribution in a PWR reactor based on neutron flux measurements at fixed reactor incore detectors. *Ann. Nucl. Energy* 90, 148–156. doi:10.1016/j.anucene.2015.12.002
- Geman, S., Bienenstock, E., and Doursat, R. (1992). Neural networks and the bias/variance dilemma. *Neural Comput.* 4, 1–58. doi:10.1162/neco.1992.4.1.1
- Gurgen, A. (2021). *Development and assessment of physics-guided machine learning framework for prognosis system*. Ann Arbor: North Carolina State University, 181.
- Hornik, K. (1991). Approximation capabilities of multilayer feedforward networks. *Neural Netw.* 4, 251–257. doi:10.1016/0893-6080(91)90009-t
- Ikonen, T. (2016). Comparison of global sensitivity analysis methods -Application to fuel behavior modeling. *Nucl. Eng. Des.* 297, 72–80. doi:10.1016/j.nucengdes.2015.11.025
- Ma, Y., Liu, J., Yu, H., Tian, C., Huang, S., Deng, J., et al. (2022). Coupled irradiation-thermal-mechanical analysis of the solid-state core in a heat pipe cooled reactor. *Nucl. Eng. Technol.* 54, 2094–2106. doi:10.1016/j.net.2022.01.002
- Ma, Y., Tian, C., Yu, H., Zhong, R., Zhang, Z., Huang, S., et al. (2021b). Transient heat pipe failure accident analysis of a megawatt heat pipe cooled reactor. *Prog. Nucl. Energy* 140, 103904. doi:10.1016/j.pnucene.2021.103904
- Ma, Y., Yang, X., and Liu, Y. (2021a). Reactivity feedback characteristic and reactor startup analysis of megawatt heat pipe cooled reactor[J]. *Atomic Energy Sci. Technol.* 50, 213–220. doi:10.7538/yzk.2021.zhuankan.0121
- McClure, P., Poston, D., and Rao, D. (2015). *Design of megawatt power level heat pipe reactors[R]*. Los Alamos: Los Alamos National Lab.

networks and other algorithms in the future. Applying the neural network in scenarios that do not require high interpretability is more advantageous.

Data availability statement

The raw data supporting the conclusion of this article will be made available by the authors, without undue reservation.

Author contributions

YL: Methodology, software, writing—original draft. MH: Investigation, formal analysis. CP: Conceptualization, methodology, supervision. ZD: Software, Writing—original draft. ZW: Formal analysis.

Funding

The work described in this paper was supported by the Sichuan Province's Outstanding Young Scientific and Technological Talent Project (2021JDJQ0034) and Science and Technology Innovation Team Program of Key Laboratory of NPIC (ZDSY-CXTD-21-04-001).

Conflict of interest

The authors declare that the research was conducted in the absence of any commercial or financial relationships that could be construed as a potential conflict of interest.

Publisher's note

All claims expressed in this article are solely those of the authors and do not necessarily represent those of their affiliated organizations, or those of the publisher, the editors and the reviewers. Any product that may be evaluated in this article, or claim that may be made by its manufacturer, is not guaranteed or endorsed by the publisher.

- Song, S. (2002). Heat balance test for determined reactor core power. *Nucl. Power Eng.* 23, 82–86. doi:10.3969/j.issn.0258-0926.2002.02.018
- Sterbentz, J. W., Werner, J. E., and Mckellar, M. G. (2017). *Special purpose nuclear reactor (5MW) for reliable power at remote sites assessment report[R]. Idaho Falls, United States: Idaho National Lab.*
- Wan, A., Dunlap, L., Ho, D., Jihan, Y., Lee, S., and Jin, H. (2020). NBDT:Neural-Based decision trees arXiv. arXiv (USA), 14.
- Xi, X., Xiao, Z. J., Yan, X., Li, Y. L., and Huang, Y. P. (2013). The axial power distribution validation of the SCWR fuel assembly with coupled neutronics-thermal hydraulics method. *Nucl. Eng. Des.* 258, 157–163. doi:10.1016/j.nucengdes.2013.01.031
- Zhang, X. Y., Trame, M. N., Lesko, L. J., and Schmidt, S. (2015). Sobol sensitivity analysis: A tool to guide the development and evaluation of systems pharmacology models. *CPT pharmacometrics Syst. Pharmacol.* 4, 69–79. doi:10.1002/psp4.6
- Zhong, R., Ma, Y., and Deng, J. (2021). Reactor startup characteristics of heat pipe cooled reactor with multiple Feedback Mechanism[J]. *Nucl. Power Eng. S2*, 104–108. doi:10.13832/j.jnpe.2021.S2.0104
- Zhou, Z. H. (2016). *Machine learning*. Beijing: Tsinghua University Press.